Impact of Ion Energy and Yield in Oblique Ion Beam Etching Process for Blazed Gratings

T. Reiter[1]*, A. Toifl[2], S. W. Kong[3], A. Hössinger[2], and L. Filipovic[1]
[1]Christian Doppler Laboratory for Multi-Scale Process Modeling of Semiconductor Devices and Sensors,
Institute for Microelectronics, TU Wien, 1040 Vienna, Austria
[2]Silvaco Europe Ltd., St Ives, Cambridgeshire, PE27 5JL, United Kingdom
[3]Silvaco Inc., Santa Clara, 4701 Patrick Henry Drive, CA, USA
*Email: reiter@iue.tuwien.ac.at

2024 International Conference on Simulation of Semiconductor Processes and Devices (SISPAD) | 979-8-3315-1635-2/24/$31.00 ©2024 IEEE | DOI: 10.1109/SISPAD62626.2024.10733316

***Abstract*—We present a model for oblique ion beam etching (IBE) processes which are applied in the fabrication of optoelectronic devices, such as blazed gratings. Our model combines top-down Monte Carlo flux calculation and the Level-Set method to accurately capture the intricate etch profile evolution during the IBE process. We demonstrate the capability of our model by reproducing experimental etch profiles presented by Zhang et al. [1]. Furthermore, we study the impact of the ion energy and yield on the time evolution of etch profiles, highlighting their crucial roles in shaping the final device geometries.**

***Index Terms*—Ion beam etching, Process simulation, Blazed gratings, Optoelectronics**

I. Introduction

Ion beam etching (IBE) is often used in the fabrication of optoelectronic devices, such as blazed gratings [2], due to its ability to precisely shape intricate microstructures with high fidelity [1], [3].

IBE involves the bombardment of a substrate surface with energetic ions, typically accelerated to high velocities. These ions interact with the substrate material, causing sputtering (physical ejection of atoms from the surface). The local sputtering rate, also referred to as yield, is influenced by several factors, including the energy of the incident ions, the angle of incidence, and the material properties of the surface. Precise control over the sputtering process allows for detailed patterning and etching of the substrate, which is essential for microfabrication and nanotechnology applications.

Zhang et al. [1] recently presented a novel method for fabricating blazed gratings using IBE. Blazed gratings are essential components in optoelectronics, that enhance the directionality and efficiency of light diffraction, making them invaluable in various high-precision optical applications. The proposed fabrication method comprises two steps: An asymmetrical native substrate grating mask (ANSGM) is generated by depositing a photoresist mask onto a silica substrate and etching at an oblique angle of 10°. Following the removal of any remaining resist residues after this step, the ANSGM is then etched at a 54° oblique ion angle to form triangular blazed gratings. This way, the blaze angle can be precisely controlled by adjusting the incident angle of the ion beam in the second etch step.

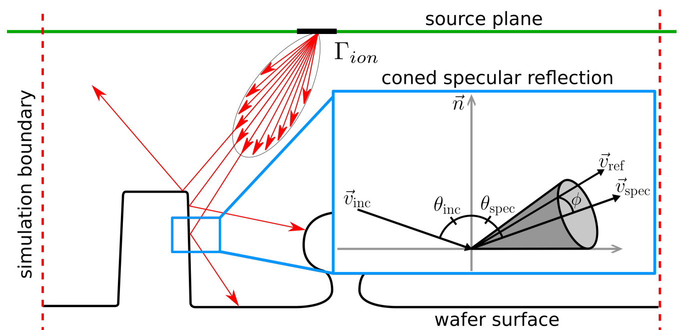

Fig. 1. Ion trajectories are traced from their initial position on the source plane, following an initial direction distribution Γ_{ion}. Upon reaching the surface, ions undergo reflection characterized by a coned distribution, with the reflected direction $\vec{v}_{\text{ref}}$ selected from a cone centered around the direction of the ideally specular reflection $\vec{v}_{\text{spec}}$.

This work presents a process model for oblique IBE, which is validated against experimental results published by Zhang et al. [1], confirming the accuracy and predictive capability of the model. Using this model, we investigate the impact of ion yield variations as influenced by energy levels and incidence angles.

II. Model

We employ a top-down Monte Carlo (MC) ray tracing approach to analyze the distribution of ion flux on the wafer surface. This approach involves partitioning the total ion flux among numerous pseudo-particles, and tracing their trajectories, starting from a source plane above the structure and possibly reflecting from the surface (cf. Fig. 1). In our simulation framework, we consider the feature scale, that is, the space close to the wafer surface. We assume ballistic transport conditions, and hence the pseudo-particles can be considered independent of each other. Under these transport conditions, we can employ ray tracing, a computational technique that efficiently calculates ray-geometry intersections. This method allows us to trace a large number of pseudo-particles, significantly enhancing the accuracy of our simulations by capturing detailed interactions and trajectories. The efficiency of ray tracing enables us to perform these precise calculations with manageable computational resources.

The IBE flux model assumes that a single-ion particle species is being accelerated towards the surface. Each ion is assigned an initial energy and direction upon creation on the source plane. The initial energies follow a normal distribution, characterized by a mean energy value and an energy variance, thus allowing for stochastic variations in the initial energy states of the ions. We utilize a tilted source distribution for the initial ray directions to take into account the tilt beam angle with respect to the wafer. This distribution is characterized by both a tilt angle and a focus angle around the principal direction. The focus angle describes the divergence or spread of the initial ion directions from the principal direction. This ensures realistic ion trajectories within our simulation framework.

An energy and angle-dependent yield is computed upon impact with the surface, contributing to the local etch rate. The yield is expressed as

$$Y(E,\theta) = \left(\sqrt{E} - \sqrt{E_{th}}\right) f(\theta), \tag{1}$$

where E denotes the ion energy and θ its incident angle relative to the surface normal. E_{th} is the material's threshold energy for physical sputtering, which is taken from literature as 20 eV for silica [4]. The function $f(\theta)$ characterizes the angular dependence of the yield and usually exhibits a maximum at some off-normal incidence angle and declines to zero at grazing angles, as shown in Fig. 2a. This material-dependent function is often fitted to the empirical form [5], [6]

$$\tilde{f}(\theta) = \sum_{n=1}^{4} a_n \cos^n(\theta), \tag{2}$$

with four parameters a_n. The angle dependence is usually normalized to obtain the value 1 at normal incidence by $f(\theta) = \tilde{f}(\theta)/\sum_{n=1}^{n} a_i$.

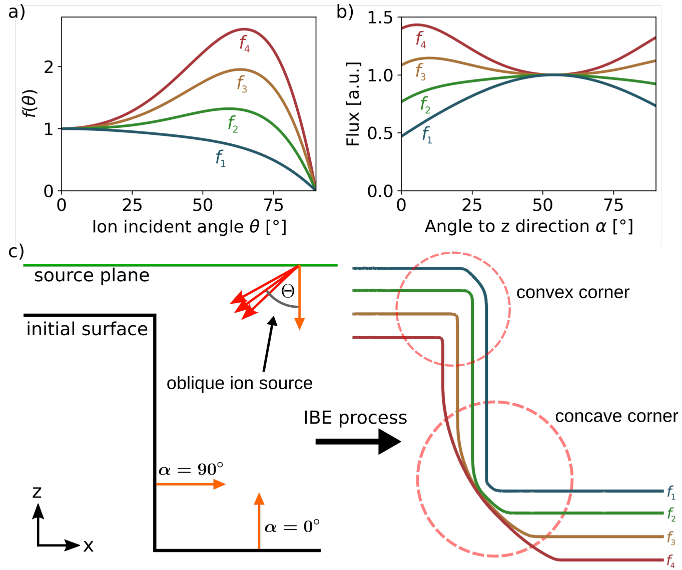

Fig. 2. Impact of yield angle-dependence during the etching process of a test structure featuring both convex and concave corners at an oblique etching angle of 54°. Four variations in the angular dependence of the yield function are visualized in Fig. a, while Fig. b demonstrates the resulting flux on the surface, which is proportional to the surface etch rate. The resulting surfaces in an IBE process using these four different variations are shown in Fig. c.

Furthermore, the ions can also undergo reflection from the surface. The functional form of the reflected energy and angle distribution is chosen to reproduce experimental observations and results of molecular dynamics simulations of ion scattering on the surface [7]. The loss of ion energy during reflection is modeled by scaling the current ion energy with a factor E_{ref} $(0 \leq E_{\mathrm{ref}} \leq 1)$ which depends on the angle of incidence θ and is manipulated by the inflection angle $\theta_{\mathrm{inflect}}$ and the exponent n. Specifically, E_{ref} is given by [8]

$$E_{\mathrm{ref}}(\theta) = \begin{cases} 1-(1-A)\dfrac{\pi/2-\theta}{\pi/2-\theta_{\mathrm{inflect}}} & \theta \geqslant \theta_{\mathrm{inflect}} \\ \mathrm{A}\left(\dfrac{\theta}{\theta_{\mathrm{inflect}}}\right)^n & \theta < \theta_{\mathrm{inflect}} \end{cases}, \tag{3}$$

where $A = (1+n(\pi/(2\theta_{\mathrm{inflect}})-1))^{-1}$ ensures that the function is continuous and smooth across $\theta_{\mathrm{inflect}}$.

The angular dispersion of reflected ions is characterized by a cosine function centered around the direction of specular reflection defined by θ_{spec}, as shown in the inset of Fig. 1, and defined as

$$\mathrm{P}(\phi) \propto \begin{cases} \cos\left(\frac{\pi}{2}\frac{\phi}{\pi/2-\theta_{\text{spec}}}\right) & \theta \leqslant \theta_{\min} \\ \cos\left(\frac{\pi}{2}\frac{\phi}{\pi/2-\theta_{\min}}\right) & \theta > \theta_{\min} \end{cases}, \tag{4}$$

where ϕ denotes the opening angle of the cone around the specular direction. This reflection process distinguishes between ions approaching the surface at grazing angles undergoing nearly perfect specular reflection and those striking the surface perpendicularly, resulting in almost diffuse reflection. Additionally, a minimum cone angle, denoted by $\theta_{\min}$, is specified to ensure a minimum spread in the reflected directions for near-grazing ions.

To simulate the time evolution of the etch profile, we employ the Level-Set method [9]. This method implicitly represents the surface by assigning each point in space $\vec{x}$ its distance from the surface $\mathcal{S}$, where the points within the volume enclosed by the surface $\mathcal{S}$ obtain a negative distance value. The resulting signed distance function $s(\vec{x})$ describes the surface $\mathcal{S}$ as the zero level set:

$$\mathcal{S} = \{\vec{x}\colon\ s(\vec{x}) = 0\} \tag{5}$$

Propagating the etch front over time involves calculating the surface's ion flux using the previously described model and solving the Level-Set equation with a velocity field $v(\vec{x})$ proportional to the computed flux distribution:

$$\frac{\partial s(\vec{x},t)}{\partial t} + v(\vec{x})|\nabla s(\vec{x},t)| = 0 \tag{6}$$

The velocity field $v(\vec{x})$ indicates the rate of change in the normal direction of the surface at each point. Solving the Level-Set equation (6) is achieved by discretizing the Level-Set function $s(\vec{x})$ on a regular grid and applying a finite difference scheme.

III. Results

A. Blazed Grating Etch

The IBE model was first calibrated to accurately reproduce the blazed grating geometry presented by Zhang et al. [1]. The model was implemented in Silvaco's Victory Process, a process simulator employing the Level-Set method and top-down Monte-Carlo ray tracing. In our simulation, we focus on the second etch step following the initial formation of the ANSGM on the silica substrate. This step involves an oblique IBE at an ion beam angle of 54°, carefully selected to optimize the etching process to achieve the desired grating profile. The calibrated model parameters, which are detailed in Table I,

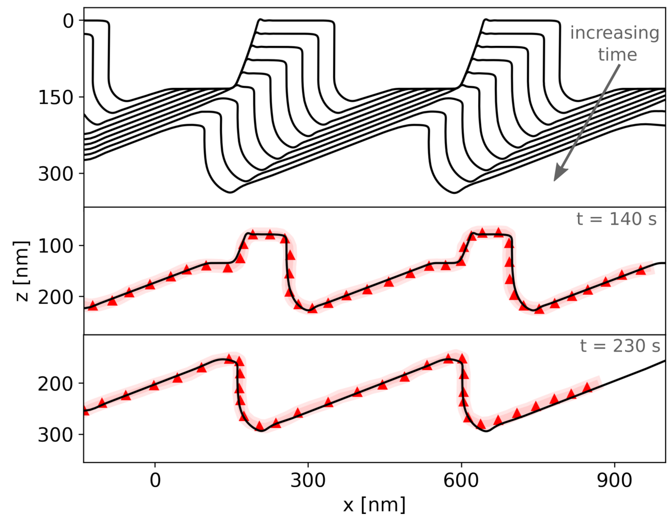

Fig. 3. Simulation results for the blazed grating etch step are depicted, with the corresponding model parameters displayed in Table I. The angle-dependence function for this simulation is visualized in Fig 2a as f_3. The black line shows the simulated profile, while the red markers represent the experimental profile extracted from the SEM image in [1].

TABLE I
Calibrated parameters of the IBE model. The parameters were calibrated to match the final surface profiles as reported in [1].

Parameter	Description	Value
E_{mean}	Mean ion energy	250 eV
E_{var}	Ion energy variance	10 eV
a_1	Parameters for yield angle dependence $f(\theta)$	1.075
a_2		-1.55
a_3		0.65
a_4		0
n	Energy reduction exponent	10
θ_{inflect}	Inflection angle	89°
$\theta_{\min}$	Minimum cone angle	5°

and the resulting etch profiles, illustrated in Fig. 3, show excellent agreement between our calibrated IBE model and the final geometry of the blazed grating. This close match validates the accuracy of our model, indicating its potential for precisely predicting the etching process.

B. Effect of Angular Dependence

We investigated the impact of variations in the angular dependence of the yield $f(\theta)$ on the propagation of the etch profile. Variations in $f(\theta)$ cause significantly different results for convex and concave corners within the etched surface. This difference arises from the adjustment of the function by the oblique etching angle. By investigating the resulting surface velocity distribution, where each surface normal is characterized by its angle to the vertical z-axis α, we observe the emergence of two distinct peaks, shown in Fig. 2b. In convex corners, an initially sharp corner will remain sharp only if there is a local minimum in the surface velocity. This occurs because both the vertical and horizontal planes etch more rapidly than the tilted planes, allowing the corner to maintain its sharpness. In contrast, in concave corners, planes with angles corresponding to the local minimum in the surface velocity are gradually formed during the etch process.

C. Effect of Ion Energies

By dividing the total flux arriving at a surface point into primary and secondary components, we can better investigate the influence of initial ion energies. The primary flux consists of ions originating directly from the source plane, which is meant to represent the ion flux arriving from the chamber immediately above the wafer. The secondary flux comprises reflected ions, which have undergone an energy reduction as described above. It is important to note that the influence of secondary fluxes captures non-local effects and extends beyond local surface orientations, as it strongly depends on the geometry around a specific surface point. Our analysis, depicted in Fig. 4, reveals that the secondary flux predominantly focuses on concave corners, leading to elevated etch rates there. Hence, the secondary flux reaching concave corners counteracts the tendency to form etch planes, as visualized in Fig. 2c. This effect is essential to achieve the characteristic acute angle at the bottom part of the blazed grating. Additionally, we observe that the mean initial ion energy determines the contribution of the secondary flux to the total incident flux. Consequently, by adjusting the mean ion energy, one can increase the etch rates in the concave corner, facilitating precise control over the etching process.

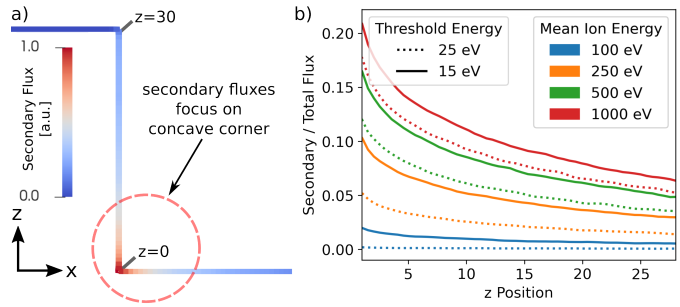

Fig. 4. Fig. a illustrates the secondary flux distribution on the convex-concave test geometry, while Fig. b presents the ratio of flux attributed to secondary fluxes. The contribution is measured along the sidewall of the test geometry, progressing from the bottom to the top.

IV. Conclusion

We have developed and validated an IBE model by comparing its predictions with experimental results of blazed grating fabrication. Using this calibrated model, we examined how the ion energy and yield angle dependence affect the propagation of the etch front. Our findings indicate that a specific yield angle dependence is crucial for achieving sharp convex corners in the final etch profile. Additionally, the ion energy must be sufficiently high so that reflected ions, which concentrate on concave corners, retain enough energy to etch these areas and preserve their shape. These insights can inform the future design and optimization of IBE fabrication setups, leading to improved precision and efficiency in microfabrication and nanotechnology applications.

Acknowledgment

Financial support by the Federal Ministry of Labour and Economy, the National Foundation for Research, Technology and Development, and the Christian Doppler Research Association is gratefully acknowledged.

References

[1] D. Zhang, X. Mao, and L. Zeng, "Blazed gratings with both controllable blaze angle and anti-blaze angle fabricated by using a twice oblique ion beam etching method,", Appl. Opt., vol. 61, pp. 9972–9978, 2022.

[2] J. Ga, P. Chen, L. Wu, B. Yu, and L. Qian, "A review on fabrication of blazed gratings", J. Phys. D: Appl. Phys., vol. 54, pp. 1–13, 2021.

[3] P. Li *et al*, "Recent advances in focused ion beam nanofabrication for nanostructures and devices: fundamentals and applications", Nanoscale, vol. 13, pp. 1529–1565, 2021.

[4] E. Gogolides, P. Vauvert, G. Kokkoris, G. Turban, and A. G. Boudouvis, "Etching of SiO_2 and Si in fluorocarbon plasmas: A detailed surface model accounting for etching and deposition", J. Appl. Phys., vol. 88, pp. 5570-–5584, 2000.

[5] E. J. Klein, and W. F. Ramirez, "Consideration of local shadowing and ion beam voltage effects in the prediction of a surface evolving under ion milling" J. Vac. Sci. Technol. A, vol. 18, pp. 166-–175, 2000.

[6] J.P. Ducommun, M. Cantagrel, and M. Marchal, "Development of a general surface contour by ion erosion. Theory and computer simulation", J. Mater. Sci., vol. 10, pp. 52-–62, 1975.

[7] B. A. Helmer, and D. B. Graves, "Molecular dynamics simulations of Ar^+ and Cl^+ impacts onto silicon surfaces: Distributions of reflected energies and angles" J. Vac. Sci. Technol. A, vol. 16, pp. 3502-–3514, 1998.

[8] R. J. Belen, S. Gomez, M. Kiehlbauch, D. Cooperberg, and E. S. Aydil, "Feature-scale model of Si etching in SF_6 plasma and comparison with experiments" J. Vac. Sci. Technol. A, vol. 23, pp. 99-–113, 2005.

[9] J. A. Sethian, "Level Set Methods and Fast Marching Methods: Evolving Interfaces in Computational Geometry, Fluid Mechanics, Computer Vision, and Materials Science", 2nd Edition, Cambridge University Press, Cambridge, U.K., 1999.